Fluid migration during contact metamorphism: the use of oriented fluid inclusion trails for a time/space reconstruction

M. CATHELINEAU*, M. LESPINASSE*†, A. M. BASTOUL*‡, C. BERNARD*†, AND J. LEROY†

*CREGU and CG CNRS-CREGU, BP 23, 54500, Vandoeuvre-les-Nancy, France
†Laboratoire d'étude des systèmes hydrothermaux, Nancy I University, Vandoeuvre-les-Nancy, France
‡Université de Marakech, Morroco

Abstract

Microthermometric characteristics of metamorphic to hydrothermal fluids and microfracturing were studied in a contact zone between metamorphic series and peraluminous granites, located in the southern part of the Mont Lozère pluton (Massif Central, France). Four major stages of fluid production or migration have been recognized: (1) N_2–CH_4 ($\pm CO_2$)-rich fluids related to the metamorphism of the C-bearing shales, occurring as fluid inclusion along the quartz grain boundaries; (2) CO_2–CH_4–H_2O vapours or liquids, with homogenization temperatures of 400 ± 20 and 350 ± 50 °C respectively, related to the first hydrothermal stage produced by the late peraluminuous intrusions; (3) aqueous fluids having low salinities and Th in the range 150–330 °C; (4) low-temperature aqueous fluids.

It is shown that the percolation of hydrothermal fluids occurs through a dense set of microfissures on a microscopic scale. The different stages of fluid percolation have been investigated by relating the deformational events to the observed fracturing. The nature of the hydrothermal fluid has been deduced by studying the trails of fluid inclusions. Analysis of the relationships of the fluid inclusion trails (F.I.T.) with structures associated with plastic deformation show that their propagation is independent of the intracrystalline anisotropies. Combined studies of their orientation in space and their microthermometric characteristics show that: (1) according to the direction, several generations of fluids are distinguished within each sample on the basis of their physical–chemical characteristics; they correspond to different stages of the hydrothermal activity and to different directions of microcrack opening; (2) in bulk isotropic media (granite), fluid inclusion trails are essentially mode I cracks which can be used as excellent markers of paleostress fields; however, in bulk anisotropic media (quartz lenses in mica schists) the migration directions of the fluids are mostly dependent on the local reorientations of the stress fields.

The study of the contact zone between granites and a metamorphic series submitted to local abnormal heat flows shows that fluid characteristics are significantly different in the two environments. Migration of carbonic fluids from mica schists towards granites occurred but is relatively limited, whilst aqueous fluids mixed in variable amounts with carbonic fluids in the metamorphic zone.

KEYWORDS: fluid migration, contact metamorphism, fluid inclusion trails, Mont Lozère pluton, France.

Introduction

THERE are relatively few data on the fluid migration and production in zones affected by regional to contact metamorphism. Thus, if the mineralogical changes occurring in intruded metamorphic series are relatively well described and understood (Goldschmidt, 1911; Tilley, 1924; Seki, 1961; Hollister, 1969) the nature of the produced fluids as well as the geometry of their migration is much less well documented, as pointed out by Roedder (1984). However, contact metamorphism of sedimentary series frequently yields fluids rich in carbon dioxide, methane or nitrogen (Bastoul, 1983) displaying similarities with fluids from diagenetic to regional metamorphic processes (reviews in Touret, 1977; Roedder,

Mineralogical Magazine, June 1990, Vol. 54, pp. 169–82

1984; Hollister and Crawford, 1981). Such fluids may play a role at least in the mass and heat transfer related to the fluid convection resulting from the intrusion, but also in the buffering of some physical–chemical parameters such as the f_{O_2} which is an important factor controlling the metal transport and/or deposition. Thus, three topics have been particularly studied in a granite/metamorphic series contact zone located on the southern border of the Mt-Lozère batholith (south-eastern French Massif Central): the changes in the physical–chemical conditions occurring between the stages of regional and contact metamorphism affecting the metamorphic series, the geometry of the fluid pathways at a given stage of the fluid migration, the degree of fluid exchange in the contact zone, and consequently the effects of contrasted physical–chemical conditions prevailing on both sides of the contact. Fluid production and circulation have been investigated by characterizing the paleo-open space geometry and the determination of the *P–V–T–X* properties of fluids trapped in healed microcracks.

Methodology

Methodological approach

Analysis of crack initiation, propagation, morphology, density and orientation in relation to local stresses has been carried out by numerous authors (see a review by Krantz, 1983). Experimental studies (e.g. Brace and Bombolakis, 1963; Friedman and Logan, 1970; Peng and Johnson, 1972; Tapponier and Brace, 1976; Krantz, 1979*a*,*b*, 1983) indicate that most cracks appear to be extensional fractures propagated roughly normal to the local maximum tensile stress axis (mode I cracks).

Microfissuring is expressed by unhealed or healed cracks (trails of fluid inclusions). After Simmons and Richter (1976), a distinction was made between intergranular (cutting across grain boundaries) and intragranular cracks (contained totally within the grain). In most cases, cracks are partially to completely filled with secondary minerals or fluid inclusions. The fluid inclusion trails (F.I.T.) (Hicks, 1884; Van Hise, 1890) appear as rectilinear succession of secondary fluid inclusions (Roedder, 1962, 1984). Tuttle (1949), Wise (1964), and more recently Lespinasse and Pécher (1986), Kowallis *et al.* (1987), Laubach (1989), and Ren *et al.* (1989) have emphasised the use of FIT for relating the different stages of fluid percolation to a regional succession of deformational events. By studying microthermometric properties of the fluids trapped in the trails, Pécher *et al.* (1985) have correlated the nature of the percolating fluid to specific directions of microfissuring and stress orientation. A similar approach has been followed in this study.

Analytical methods

A thick and a thin section have been oriented and realized on the same fragment of each sample. Systematic measurements of microfissures have been carried out on each section. Analysis of the microfissures takes into account different parameters such as the nature of the crack, the type of cross-cut mineral and the density of each crack family. As microcracks and fluid inclusion trails are microstructural markers, data were compared with the results of the stress field reconstruction obtained by using the data measured on striated faults and computer simulations (Etchecopar *et al.*, 1981; Etchecopar, 1984).

Fluid inclusions have been systematically studied in healed microcracks from the granite quartz grains. Each F.I. was studied with respect to the microstructural context. The very small size, around 5 μm, of the fluid inclusions makes the study of several inclusions within the same F.I.T. difficult. Thus, results are not presented trail by trail but gathered together for a given direction of F.I.T.

Microthermometric characterization of the fluids was performed on oriented fluid-inclusion wafers (300 μm thick) using a heating–freezing Chaixmeca stage (Poty *et al.*, 1976). Salinity, expressed in equivalent NaCl, and fluid density of gas-free fluid inclusions in quartz, were determined by microthermometry (Potter, 1977; Potter *et al.*, 1978). In gas-bearing fluid inclusions, CH_4 was identified by liquid–vapour equilibria below $-81\,°C$ and CO_2 by melting of a solid below $-56.6\,°C$. The volumetric fraction of the aqueous liquid (Flw) and the volumetric fraction of the carbon rich liquid in the carbon-rich phase (Flc) have been estimated at room temperature by reference to the volumetric chart of Roedder (1972). Molar fractions of CO_2, CH_4, H_2S and N_2 were determined in individual inclusions by micro-Raman analysis performed on a DILOR X–Y multichannel modular Raman spectrometer.

f_{O_2} was calculated from the P–V–T–X properties of individual inclusions in the C–O–H–S system (Dubessy, 1984; Ramboz *et al.*, 1985; Dubessy *et al.*, 1987, 1989).

Materials

Geological setting of the studied area

The study area is located in the southern part of the French Massif Central (Fig. 1), on the western border of the Mont Lozère batholith. Fig. 1*b* and 2 show the different geological units of

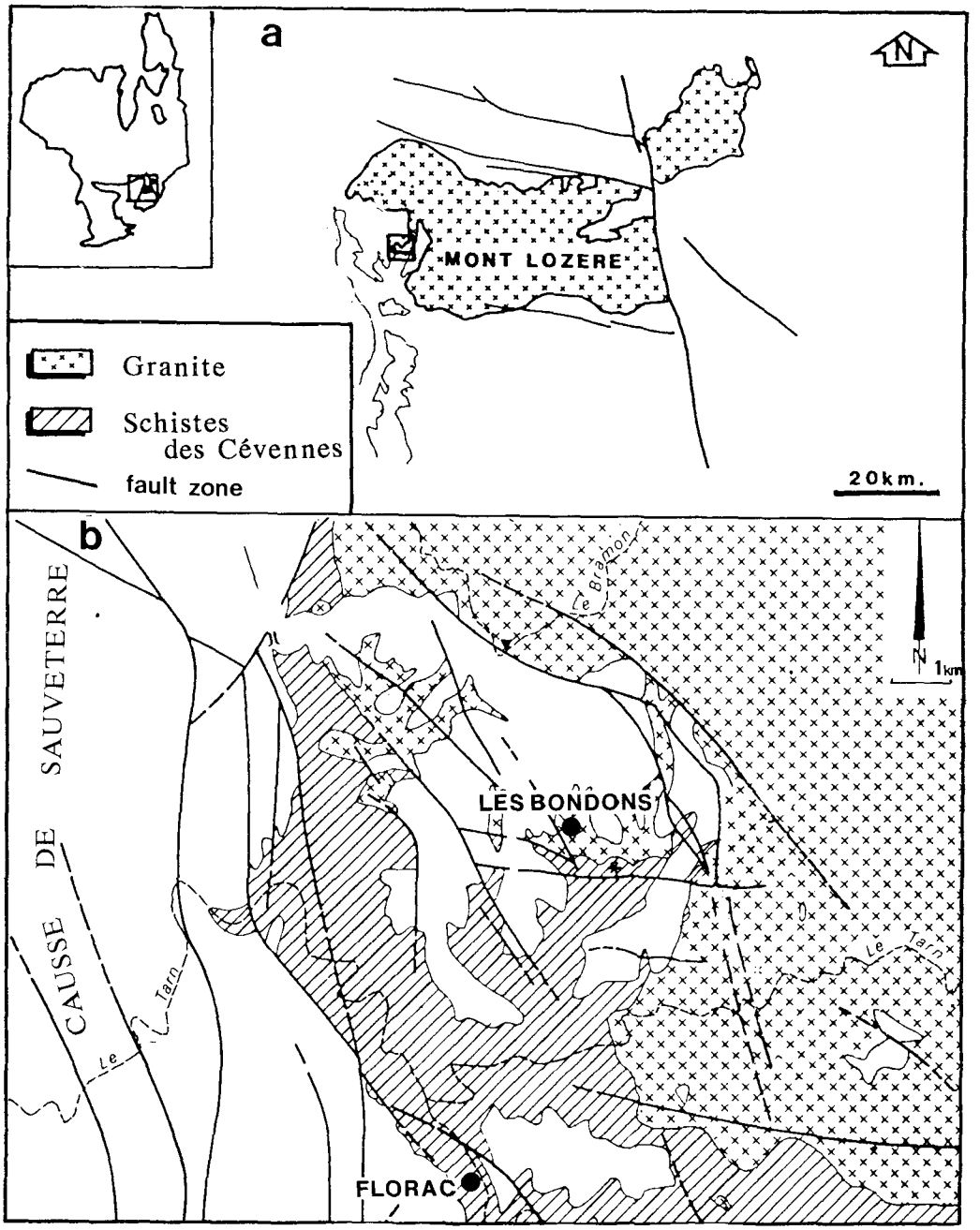

FIG. 1. Sketch map of the southern part of the French Massif Central: (*a*) Mt-Lozère batholith; (*b*) Les Bondons area.

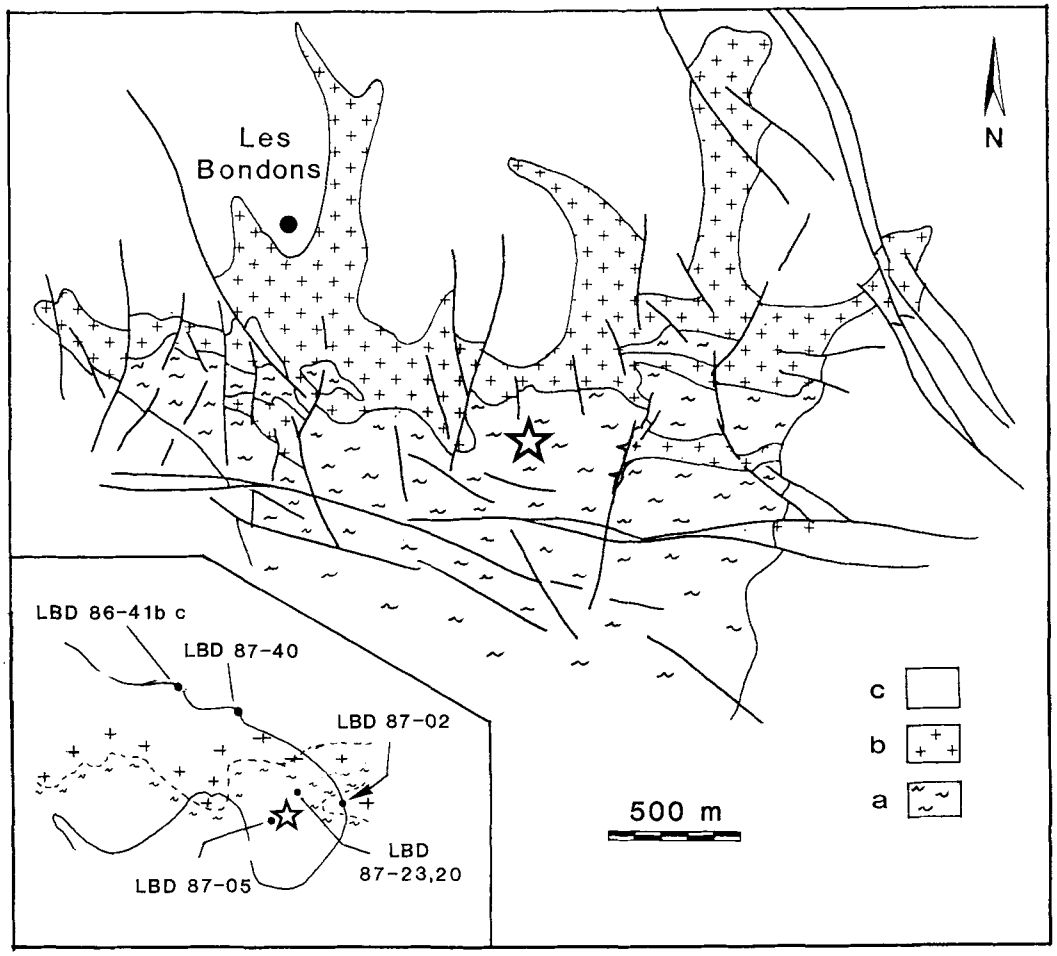

FIG. 2. Location of the studied area: (*a*) Paleozoic series; (*b*) Mont Lozère granite batholite; (*c*) sedimentary cover (after Virlogeux, 1984).

the contact zone: the Palaeozoic metamorphic series composed of mica schists and black shales which are affected by the regional Hercynian metamorphism, the Bondons peraluminuous granite which is a 2-mica facies of the Mont Lozère batholith, and a series of intrusive aplites which crosscut the contact and occur as subhorizontal sills within the metamorphic layers.

Studied materials

Microstructural makers and fluids have been studied in metamorphic quartz grains or lenses from the metamorphic series, in magmatic quartz grains from the aplite sills and the Bondons granite and in some quartz veins with crosscut the different units. In most cases quartz shows relatively intense microfracturing and fluid trapping along healed microcracks. Thus, most fluid inclusions are observed as fluid-inclusion trails. A limited number of metamorphic quartz grains exhibit isolated inclusions and/or inclusions located along grain boundaries.

Structural and microstructural context of the fluid migration

Fracture and vein orientation

The facture network in the Les Bondons ore deposit is characterized by mean directions: N20°E, N80°E, N130°E and N170°E (Fig. 3*a*). These directions are in good accordance with the fracture network determined from the analysis of aerial photographs (Virlogeux, 1984) (Fig. 2). Quartz veins are orientated N–S, N70°E to N90 °E and less frequently N120°E (Fig. 3*b*).

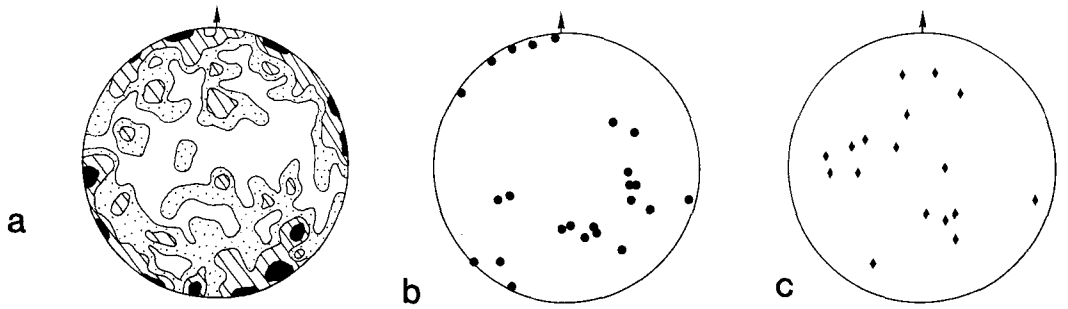

FIG. 3. Stereographic projection of fracture and vein orientations.; Schmidt diagram, lower hemisphere: (*a*) diaclase orientations: 134 data points, contours at 0.5, 1.5, 3.5 and 5%; (*b*) quartz veins, 17 data points; (*c*) aplitic veins, 17 data points.

Aplite veins display two mean directions, N0°E and N70° to N90°E (Fig. 3*c*).

Palaeostress fields

Palaeostress trajectories were determined by using a computer code (Etchecopar *et al.*, 1981; Etchecopar, 1984) which is based on Bott's theory (1959). From a data set of striated fractures initiated or reactivated in more than one tectonic phase, this code allows the effects of the main superimposed stress state to be distinguished and stress directions to be estimated. Forty-one fault planes and their striae were measured in different parts of the Les Bondons granite. Fig. 4 shows that the measured striae result from the superposition of at least three main stress tensors, characterized by an intermediate stress ($\sigma 2$), remaining close to vertical, and by maximum stress ($\sigma 1$) orientated respectively N15°E, N90°E, N120°E. The well-defined N15°E direction (Fig. 4*b*) accounts for 20 to 30% of the striated planes, and the N120°E for 20% (Fig. 4*c*). In the field, conjugate structures in relation with the N15°E compression are dextral (N170°E to N10°E) and sinistral (N40°E to N60°E) faults; N120°E compression is marked by sinistral movements in N140°E to N160°E faults and dextral movement on N70°E to N90°E faults. The identification of the N90°E compression (Fig. 4*d*) remains hypothetical as it is determined from an insufficient striae percentage (<15%). Nevertheless, results of the Les Bondons region are in good accordance with regional palaeostress fields determined around the Mont Lozère batholith (Raynaud, 1979; Lespinasse, 1981; Vergely and Blanc, 1981). Fault intersections and superimposition of striae yield the following stress chronology: N120°E, N15°E, N90°E. The homogeneity of the regional palaestress trajectories at a given stage of the deformation is noteworthy (Fig. 4).

Microfissuring

The brittle deformation is represented in the granite, as well as in the metamorphic lenses, by a set of healed F.I.T. and unhealed microcracks. Lespinasse (1984), Lespinasse and Pécher (1986) have shown that cracks, F.I.T., intra- and transgranular markers display similar networks in granites. However, some detailed works on the geometry of these markers as a function of local anisotropies have been carried out on the heterogeneous materials from the Bondons area before the systematic use of the F.I.T. as markers of microfracturing and fluid migration. The representative nature of intragranular and intergranular F.I.T. as reliable microstructural markers has been investigated.

Intragranular and intergranular F.I.T. networks

A preliminary comparison between intragranular and intergranular F.I.T. networks was made on thin sections from two granitic samples (samples LBD 87-02, LBD 87-40). Results show that no significant difference characterize the intra/intergranular F.I.T. networks (Fig. 5). This suggests that the intragranular or intergranular F.I.T. may be used indiscriminantly as microstructural markers. In addition. Fig. 6 shows that microfissuring of the two granite samples is present in three main orientations: N–S (N170°E to N10°E), NE–SW (N40°E to N60°), NW–SE (N120°E to N135°E) which are approximately comparable with the directions observed in the fracture network.

Geometry of the microstructural markers

Fig. 6 gives the results of the microfracture analysis carried out on the seven samples from the Bondons area. In the different granite samples, microstructural markers display rather

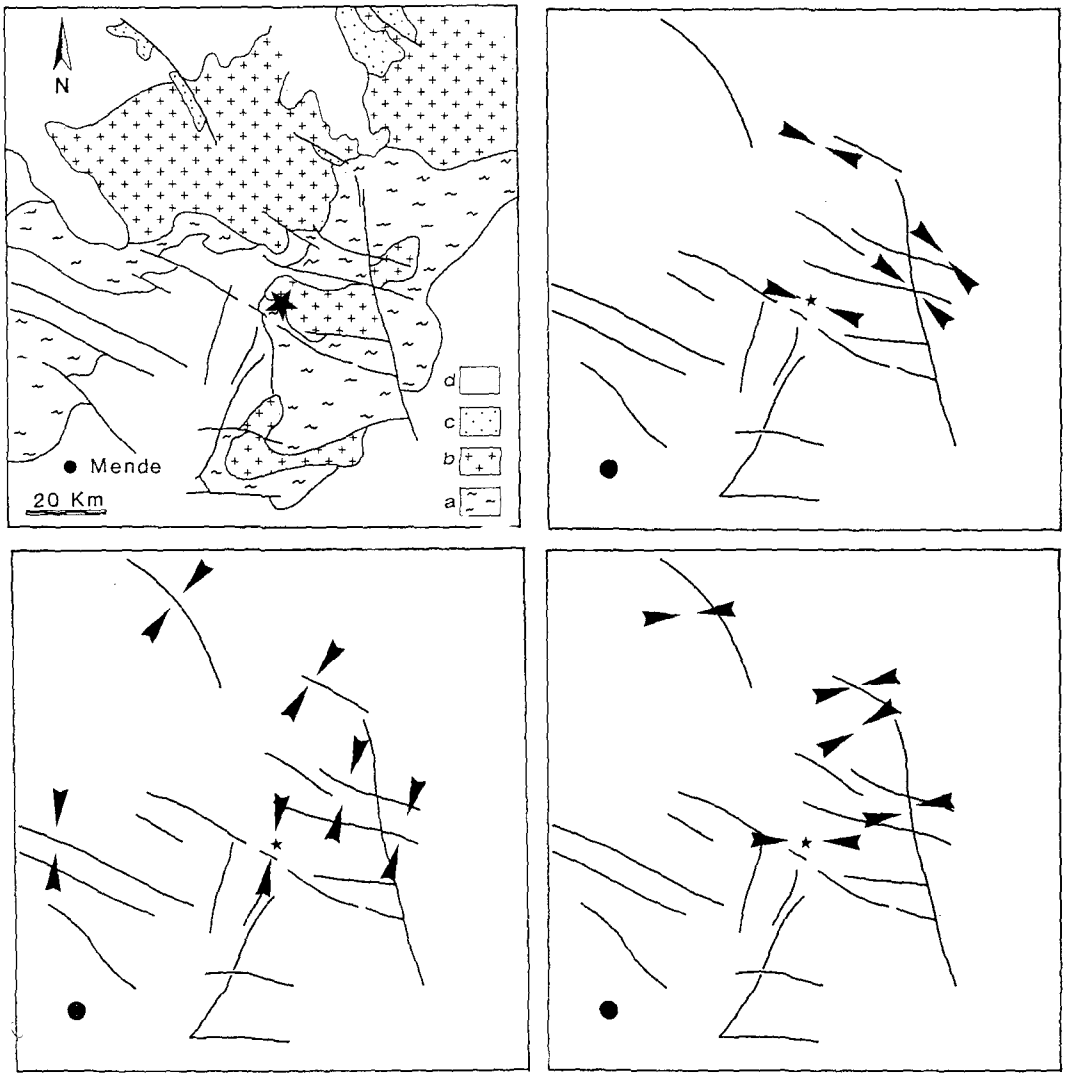

FIG. 4. Synthetic representation of the palaeostress fields in the south east of the French Massif Central; the star (*) indicates the Les Bondons location; the arrows represent the orientation of the average compressive stress tensor: (*a*) geological contex, a = Palaeozoic series, b = granites, c = sedimentary basins, d = sedimentary cover; (*b*) NW–SE compression; (*c*) NNE–SSW compression; (*d*) E–W compression.

similar preferential orientations, with slight differences in their relative numbers: N–S (N170°E to N10°E), NE–SW (N40°E to N60°E), E–W (N80°E to N100°E) and NW–SE (N120°E to N135°E). In the aplite veins (samples LBD 87–23, LBD 87–41b), microfissuring is characterized by two predominant orientations N–S and NW–SE and a less significant NE–SW direction, which are similar to those from the granite. In environments constituted of two or more lithologic units (quartz lenses within metamorphic rocks, quartz veins), F.I.T. networks display significant variations according to their location. These networks are different from the F.I.T. networks determined in the granite.

Interpretation

The microfissuring is characterized by four main orientations, N–S, NE–SW, E–W and NW–SE. It is possible that these directions are

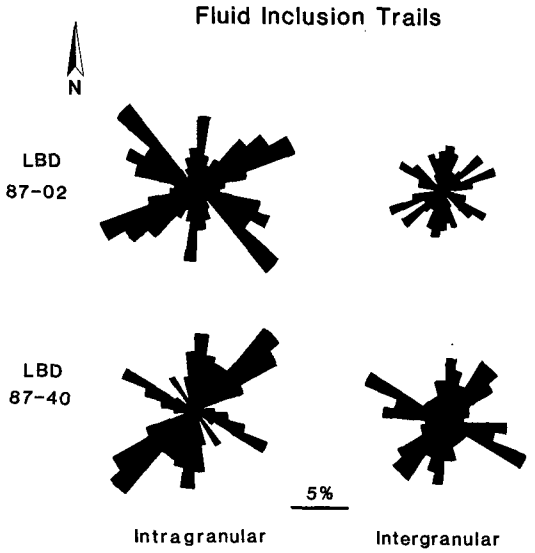

FIG. 5. Comparative analysis of the Fluid Inclusion Trails in two granitic samples (LBD 87–02, LBD 87–40); distinction was made between intragranular and intergranular networks.

related to the main compressional directions determined from the stress field analysis. In the granite samples, microfissures shows strong structural similarities suggesting the presence of a nearly homogeneous microfissure network. This supports previous results obtained on other granite massifs (Lespinasse and Pécher 1986; Lespinasse and Cathelineau, 1990) where a homogeneous crack network related to the regional compression events is observed on a large scale.

However, significant variations in orientation are observed in other lithological units than granite. The dominant NNE–SSW direction observed in sample LBD 87–05 and NW–SE in sample LBD 87–20, may indicate that the microfissuring propagation may be controlled by local heterogeneities. The presence of local anistropies results in local stress refraction during deformation, and therefore to local reorientation of the F.I.T. Consequently, relatively heterogeneous patterns of microfractures characterize complex environments, such as the metamorphic series, where discontinuities are abundant.

Fluid inclusion data

Results

Microthermometric results are summarized in Tables 1 and 3, whilst Raman microprobe analysis carried out on selected fluid inclusions are given in Table 2. Five fluid inclusion types were identified based on microscopic, microthermometric and raman spectroscopic characteristics (Bastoul, 1983; Bastoul *et al.*, 1988; Bernard, 1988).

(i) Decrepitated inclusions. Ld inclusions are decrepitated inclusions surrounded by clouds of submicroscopic inclusions and containing graphite crystals; they are found exclusively in the metamorphic area along quartz grain boundaries and within quartz lenses. Some of the Ld inclusions are associated with small-sized monophase inclusions of the type Lc (group a) defined below. The latter inclusions could represent inclusions preserved from decrepitation by their size which is three to five times smaller than the decrepitated ones.

(ii) Aquo-carbonic inclusions. Lc and Vc inclusions are carbon-rich inclusions with variable H_2O content, with homogenization of the non-aqueous part (Thc) mostly to the liquid, and total homogenization of the inclusion (TH) to the liquid or to the vapour. Lc and Vc inclusions exhibit distinct room-temperature phase relations namely apparent monophase inclusions and liquid–vapour inclusions with relatively variable liquid-to-vapour ratios. The melting temperature of the CO_2 ($TmCO_2$) is significantly lower than the Tm of pure CO_2 (Fig. 7), indicating the presence of volatile compounds other than CO_2, such as CH_4 and N_2. This is confirmed by Raman microprobe analysis. There are no significant differences between the $TmCO_2$ of carbonic fluid inclusions trapped in the granite environment or those within the metamorphic series (Fig. 7).

Three groups may be distinguished based on the microthermometric and Raman data as shown in Table 1. Thus, within the three groups *a, b, c*, $TmCO_2$ measurements have mode values at −63, −61 and −58 °C, and measurements of the Thc(L-V) for the non-aqueous phase have mode values around −90, −35 and +10 °C respectively.

CH_4 content ranges from to 75 to 10 mole % but have distinct content ranges within the three groups. N_2 has been detected by Raman probe in almost all the analysed inclusions, with a content reaching 15 mole % in group *a*. TH [TH L-V(L or V)] when available are mainly in the range 320–440 °C (Table 1).

Aqueous fluids

(iii) Ll and Vl inclusions are almost purely aqueous, with homogenization TH (L-V) to the liquid or to the vapour.

(iv) Ls1 and Ls2 inclusions are aqueous with daughter minerals (halite, or halite + an unidentified mineral) and homogenize to the liquid.

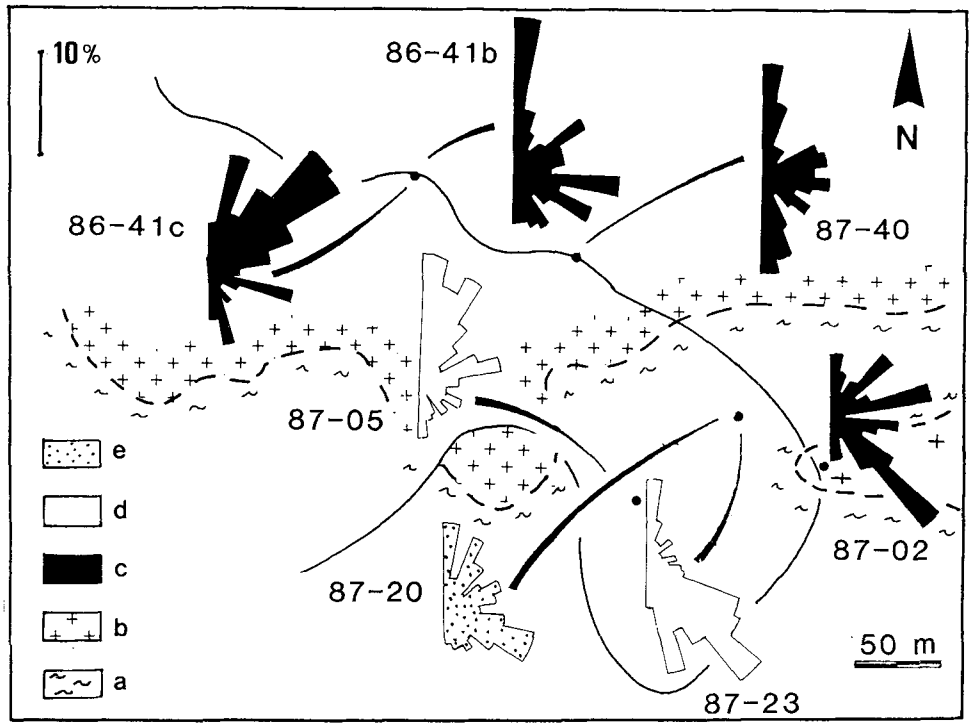

FIG. 6. Microfissuring (F.I.T. + cracks) in the granite (samples LBD 86–41c, LBD 87–40, LBD 87–02), in the quartz lenticulations (samples LBD 87–05, LBD 87–20) and in aplitic veins (samples LBD 87–23, LBD 86–41b). (*a*) Paleozoic series; (*b*) Les Bondons granite; (*c*) data on granites and intragranitic aplite; (*d*) data on the metamorphic quartz lenses; (*e*) data on the intrametamorphic aplite.

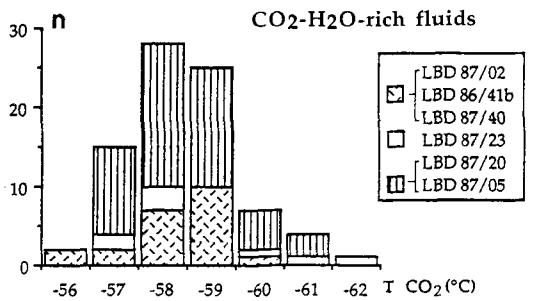

FIG. 7. Histogram of the $TmCO_2$ measured on carbonic fluid inclusions from the granite zone (samples from granite and intragranitic aplite: 87/02, 41b, and 40), from intrametamorphic aplite (87/23), and from the metamorphic series (87/05 and 20).

(v) L2 inclusions are liquids which represent the latest fluid to be trapped, since their fluid inclusion trails crosscut all the above described F.I.T.

Trails of secondary H_2O–NaCl-rich fluid inclusion (L1, V1, L2) are frequently observed in quartz veins and quartz grains from the aplite or granite, but are less abundant in the metamorphic quartz grains or lenses. Ls inclusions were found more sporadically, mostly in the metamorphic zone. The V1 inclusions were only observed in the aplite and the granite from the contact zone (sample 87–02), and saline inclusions in sample 87–05.

Microthermometric properties are given in Table 3. Three groups of inclusions displaying similar homogenization temperatures mostly ranging from 250 to 360 °C may be distinguished by their TmH_2O and type of homogenization: inclusions V, L and Ls1, Ls2. V inclusions have TmH_2O ranging from −0.5 to −2.4 °C whilst L1 inclusions are characterized by TmH_2O in the range −2 to −8 °C. No gas species (CO_2, CH_4) have been identified either by microthermometry or Raman spectroscopy within the gas phase. Ls1 and Ls2 inclusions are characterized by very low TmH_2O in the range −36.5 to −37.7 °C and −32 to −37 °C respectively whilst the melting temperature of the halite cube (Tms1) is in the range 175–195 and 170–260 °C respectively. However,

Table 1 : Representative analytical data for the different groups of carbonic fluid inclusions found in Les Bondons quartz samples.

		Metamorphic quartz lenses		Quartz vein
		group a	group b	group c
Fluid composition		**CH4-N2-(CO2 (±H2O)**	**CO2-CH4-N2 (±H2O)**	**CO2-CH4-H2O (±N2)**
mean composition	**CO2**	0	50 - 80	85-90
of the volatile phase	**CH4**	75	10 50	10 - 15
(RAMAN)	**N2**	25	0 - 30	0
	Thc (range)	-120 ,-80	-40 ,0	0 ,20
	Thc (mode)	- 90	- 35	10
Microthermometric	TmCO2(range)	-65 , -62	-68 ,-58	-58 ,-57
properties	TmCO2(mode)	- 63	- 61	- 58
	Tf H2O(range)			-8 ,-4
	TH (range)			320 ,440
	TH (mode)			340 and 400
n		53(Thc)	120(TmCO2)	180(TmCO2)
Flw		0-40	0-30	0-30

Table 2 : Interpreted bulk composition of selected fluid inclusions from the carbonaceous stages.

Incl. n°	Flw	XH2O	XCH4	XCO2	XN2	Th	Tm
17-13	0	0	71.62	0.00	28.38	-90.4V	
14 - 1	0	0	21.29	78.70	0	0 V	-62.4
14 - 1	10		15.62	57.36	0	"	"
5a - 1	0	0	9.31	90.68	0	15.2L	-59.7
5a - 1	10	35.33	5.94	58.71	0	"	"
5a-4	0	0	15.59	84.40	0	14V	-60.4
5a-4	10	32.69	10.37	56.93	0	"	"
5a-6	0	0	10.43	89.57	0	16V	-59.9
5a-6	10	32.93	6.99	60.03	0	"	"
6 - 7	10	50.03	9.56	40.42	0	7V	-59.5
6 - 7	20	68.18	5.79	26.02	0	"	"
7 - 1	0	0	8.02	63.12	28.25	7.1V	-58.7
7 - 1	10	53.52	3.52	29.83	12.41	"	"
7 - 2	20	40.5	5.6	47.23	6.64	-10.5V	-59.6
B - 9	30	55.55	13.06	25,83	5.54	-40V	-67
B - 4	20	39.51	16.54	38.54	5.3	-40V	-63.8

only Ls2 inclusions display high TH up to 300 °C, whilst TH for Ls1 are lower in the range 180–260 °C.

L2 inclusions are characterized by relatively low TH(L-V)L and TmH_2O in the range −0.2 to −3 °C.

Bulk chemical evolution

The bulk chemical compositions of the Vc, Lc inclusions is characterized by an increasing XH_2O and decreasing XCO_2 and XCH_4. These inclusions are clearly distinct in composition from the N_2–CH_4-rich inclusions which occur isolated in metamorphic lenses.

Since exceptional TH-Tm H_2O pairs were obtained for Vc and V inclusions, only a box of the representative values was drawn in the TmH_2O-TH diagram (Fig. 8). The chemical evolution as a function of decreasing TH, especially a transition from early stages dominated by volatile-rich fluids (Lc, Vc with TH above 300 °C), and stages with mixed aqueous and aquo-carbonic fluids with TH in the range 250–350 °C (Lc, Vc, L), towards stages characterized by almost purely aqueous fluids, with TH below 250 °C (L1, L2) is evident. There is a corresponding general decrease in the fluid salinity in series of the trapped aqueous liquids from high-*T* to low-*T* conditions.

The presence in the same area of aqueous vapours with very low salinities, liquids of intermediate salinities and brines, all displaying TH in the range 280–320 °C, suggests that V1 and Ls inclusions could derived from the boiling of one of the observed aqueous liquid. However, these different kinds of inclusions are not found within the same fluid inclusion trails.

P–T evolution

The *P–V–T–X* properties of every inclusion studied define an isochore in the *P–T* plan. The *P–V–T–X* properties of aquo-carbonic inclusions Vc (groups *b* and *c* for inclusions characterized by low N_2 contents) were modelled by the H_2O–CO_2–CH_4 system using the equations of Kerrick and Jacobs (1981) and Jacobs and Kerrick (1981) and the data given in Table 3. Representative isochores are given in Fig. 9.

Probable minimum pressure of trapping of the Lc (groups *a* and *b*) in earliest stages affecting the metamorphic quartz lenses is around 2–3 kbars in a temperature range of 350–400 °C, and is probably a lithostatic pressure indicative

Table 3 : Representative analytical data for the different types of aqueous fluid inclusions found in Les Bondons quartz samples.

Fluid composition		Tm H2O			TH		Tms1
(H2O-Nacl)	*range*	*mode*	*n*	*range*	*mode*	*n*	
V	-0.5,-2.4			300 -360			
L	-8 , -2	- 4	40	300 - 400	340	66	
Ls1	-36.5,-37.7			180 - 260			175-195
Ls2	-32,-37			240 - 300			170-260
L2	-3 , - 0.2	-0.5 /-2	314	150 - 300	200/260	104	

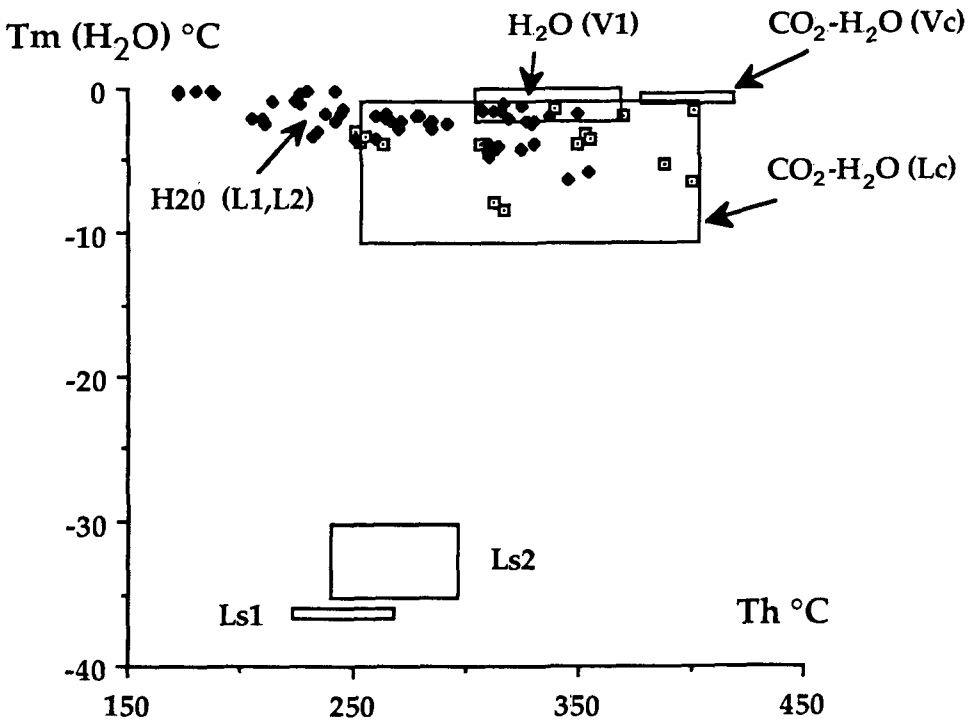

FIG. 8. Tm H_2O–TH diagram for the representative types of fluid inclusions.

of relatively deep structural levels (7–10 km depth). However, the same quartz lenses may display Vc (group *c*) inclusions displaying much lower densities and probable trapping pressures in the range 0.5–1.5 kbar. It is possible such changes illustrate the pressure drop from lithostatic to intermediate to hydrostatic conditions which occurred between the regional metamorphism stage and the contact metamorphism event. The presence of decrepitated inclusions Ld, probably of the same type than the N_2–CH_4-rich inclusions, in metamorphic lenses give evidence of this pressure drop which may have reached 1 to 2 kbar. Such pressure drop may be consecutive to the general uplift and denudation which affected the Variscan domains at the end of the Hercynian orogeny.

Decompression events suggested by the decreasing density of the trapped aquo-carbonic fluids, may have favoured the entrance of aqueous fluids within the fault system. Trapping pressures of L2 are probably intermediate between the lowest pressures given by the less dense Vc inclusions, and hydrostatic pressures. Fluid inclusion (L1, Ls1, Ls2, and then L2) trails displaying decreasing TH probably indicate successive trapping at decreasing temperatures if pressure is considered as hydrostatic.

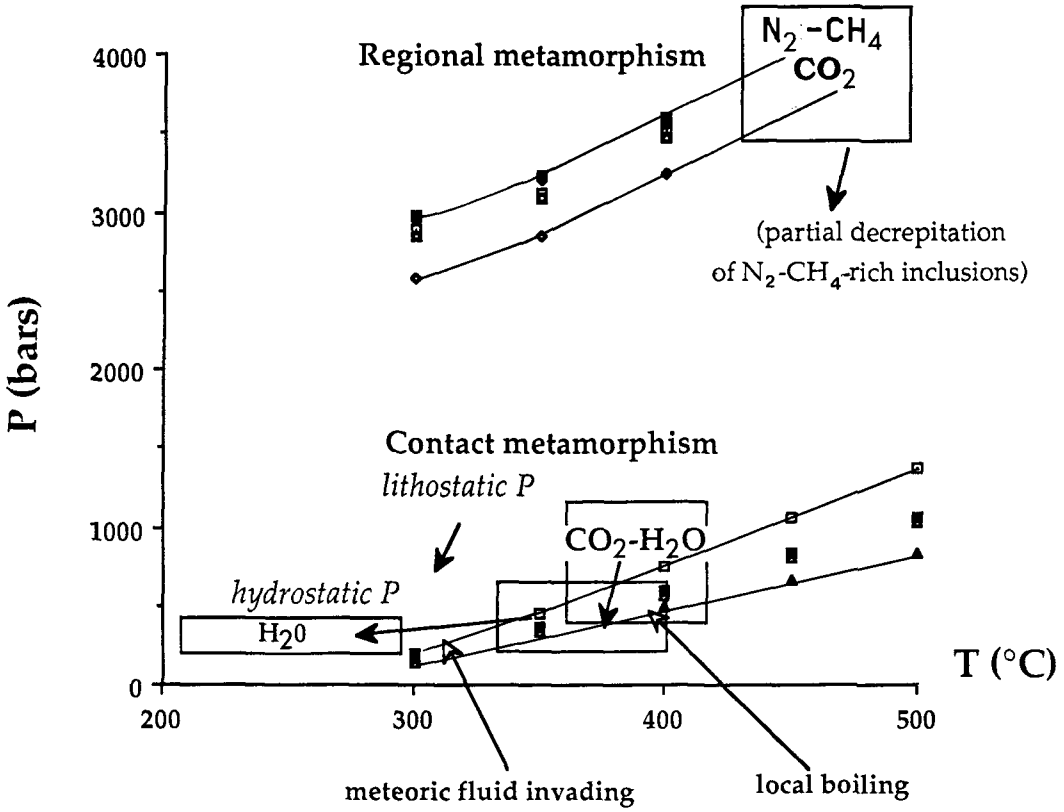

FIG. 9. Reconstruction of the *P–T* conditions during the different stages of fluid production and migration.

Estimations of pH–f_{O_2}–f_{S_2} conditions

High *P–T* chemical equilibria: the data deduced from the *P–V–T–X* properties of fluid inclusions yield an f_{O_2} estimation of $10^{-30.5 \pm 0.5}$ at temperatures around 350 ± 50 °C for Lc, Vc (type c) inclusions from metamorphic quartz lenses or from the granite sampled at a few metres from the contact zone (LBD87–02). Thus, f_{O_2} was very close to that fixed by the Ni–NiO oxygen buffer within the metamorphic zone. The small amount of carbonic fluids found in the granite samples exhibit similar compositions to those from the metamorphic rocks, indicating that fluids issued from metamorphic series which probably migrated through the first metres of the granite environment, and did not suffer significant compositional and redox state changes. On the contrary, the granite is characterized by relatively high f_{O_2} conditions, as shown by extended early hematisation and aqueous fluid migration. It is highly probable that these contrasting f_{O_2} conditions are the reason of the occurrence of small uranium concentrations in disseminated branneriites observed along the contact zone within the metamorphic area (Cathelineau, 1983). Such U concentrations may result from the reduction of the oxidizing fluids which could have leached U from the granite, by the fluids from the metamorphic environment.

Fluid pathways

Results

Geometric analysis of orientated fluid inclusion trails, characterized by fluid composition and density is shown in Fig. 10.

In the granite, aqueous liquids (L1, L2 inclusions) are dominant in N–S orientated F.I.T., but are less dominant in NE–SW and EW orientated F.I.T. Type ii (Vc, Lc) F.I.T. are not very abundant and orientated N–S (NO°) and N70–80°. In the granite contact zone, sample 87–02 displays F.I.T. mostly orientated between N60° and

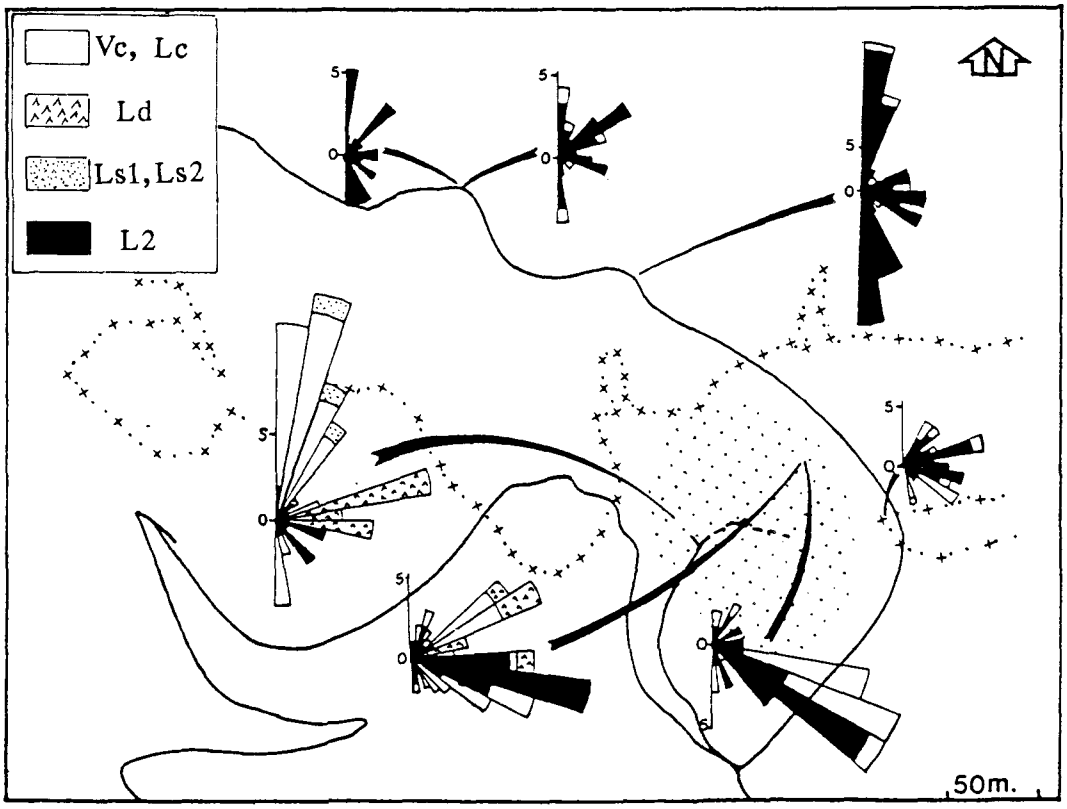

FIG. 10. Map with rose-diagrams of F.I.T. with distinction of the type of dominant fluid inclusion within the trails. Ld, decrepitated fluid inclusions; V, vapours, mostly aquo-carbonic; L, liquids, mostly aqueous liquids; Ls, aqueous liquids with daughter minerals.

N140° comprising aqueous liquids and vapours, and less abundant Lc, Vc F.I.T. with dominant orientations between N120 and N160.

In the metamorphic area, F.I.T. orientations depend on local stress anisotropies. However, given fluids are trapped in specific F.I.T. and directions on the sample scale. For instance, Ld F.I.T. are orientated N80–110°E in sample 87–05, N50–70°E and N90–100° in sample 87–20. Ls inclusions are observed in F.I.T. orientated N10°–40°E in sample 87–05. Type ii (Vc, Lc) inclusions are far more abundant than in the granite samples and hosted by F.I.T. orientated N–S (sample 87–05), NE–SW (sample 87–20), and dominantly N90°–N130°E in samples 87–20 and 87–23.

Interpretation

Fluid trapping occurred in the Bondons area by means of a complex succession of opening and reopening of the open microfracture networks. During regional metamorphism, N_2–CH_4–CO_2 rich inclusions were trapped as isolated inclusions or along grain boundaries under high *P–T* conditions. During contact metamorphic conditions, the reheating of the metamorphic series under lower pressures but relatively high temperatures caused the formation of carbonic fluids in the metamorphic area as a result of graphite–fluid equilibrium (Bastoul, 1983, Dubessy, 1986) and induced a convective fluid system. Thus, meteoric and aqueous fluids coming at least partly from the granite migrated through the contact zone towrds the metamorphic series which were intruded by the aplite sills. It is highly probable that aqueous fluids boiled in places, and that the resulting vapours and brines were trapped in locations determined by the different fluid densities of vapours and liquids, and may have led to differential migration after unmixing. Such processes have been frequently observed in geothermal systems where boiling is clearly demonstrated

(Cathelineau *et al.*, 1986). Both early and late-stage fluids migrated homogeneously in the isotropic media (granite, aplite) whilst more complicated patterns are observed within the metamorphic series.

Conclusions

This study has shown that:

(*a*) In bulk isotropic media, such as granites, the fluid inclusion trails (F.I.T.) are good microstructural markers which are probably related to the stress fields. However, it is necessary to be careful when using directions of F.I.T. in bulk anisotropic media, such as metamorphic rocks, which are characterized by numerous discontinuities yielding local stress reorientations.

(*b*) F.I.T. can be used to interpret the fluid migration, since F.I.T. may be relatively easily distinguished by the properties of individual inclusion fluid phases in healed microcrack.

(*c*) Significant changes in the physical–chemical conditions occurred in the conditions of fluid trapping in the evolution of the Bondons granite contact zone, namely: changes in the bulk chemical composition from early aquo-carbonic fluids, which are probably of metamorphic derivation, to the aqueous fluids related to the convection of meteoric fluid in relation to the intrusion and the latest events which are not related to magmatism; changes in the *P–T* conditions from early-stage trapping characterized by lithostatic pressures and relatively high temperatures at relatively deep structural levels, towards hydrothermal conditions with lower temperatures in the range 150–300 °C and intermediate to hydrostatic pressures at shallow structural levels; and changes in the factors controlling the fluid migration, which was initially induced by the metamorphism and affected by fluid convection linked to the late intrusion of peraluminous granites and to the subsequent thermal anomaly developed around the intrusive bodies.

(*d*) Significant differences characterize the fluid migration in the two environments in the vicinity of the contact zone: there are small inputs of carbonic fluids into the granites, whilst relatively large inputs of meteoric fluids, probably some of them coming from the granite, migrating through the metamorphic series.

Acknowledgements

The authors wish to express their gratitude to MM. Pfiffelmann, Bassaget, Donnadieu, Virlogeux, and Viard (CFMU-MOKTA mining company) for their technical and scientific assistance in the field and mine aspects of this paper. J. Dubessy is warmly acknowledged for his help, as well as his analytical (Raman analysis) and scientific contribution to this work.

References

Bastoul, A. (1983) Unpub. thesis Nancy I Univ., 165 pp.
——Cathelineau, M., and Cuney, M. (1988) *12 RST, Lille, Soc. Géol. Fr. Paris*, 10.
Bernard, Ch. (1988) DEA Nancy I Univ., 41 pp.
Bott, M. H. P. (1959) *Geol. Mag.* **96**, 109–17.
Brace, W. F. and Bombolakis, E. G. (1963) *J. Geophys. Res.* **68**, 3709–13.
Cathelineau, M. (1983) *C.R. Acad. Sci.* Paris, **296**, 985–8.
——Marignac C. and Puxxedu M. (1986) *5th Int. Symposium on Water Rock Interaction. Reykjavik (Islande)*, 100–3.
Dubessy, J. (1984) *Bull. Mineral.* **107**, 157–68.
——(1986) Thèse d'état Univ. Nancy I, 198 pp.
——Ramboz C., Nguyen Trun C., Cathelineau M., Charoy B., Cuney M., Leroy J., Poty B. and Weisbrod A. (1987) *Bull. Mineral.* **110**, 261–81.
——Poty, B. and Ramboz, C. (1989) *Europ. J. Mineral.* **1**, 517–34.
Etchecopar, A. (1984) Unpub. thesis, U.S.T.L. Montpellier, 260 pp.
——Vasseur, G. and Daignières, M. (1981) *J. Struct. Geol.* **3**, 51–65
Friedman, M. and Logan, J. M. (1970) *Bull. Geol. Soc. Amer.* **81**, 3417–20.
Goldschmidt, V. M. (1911) *Die Kontaktmetamorphose im Kristiangebiet. Vidensk. Shriftre.* I. *Mat. Naturv. K.*, no. 11.
Hicks, H. (1884) *J. Geol. Soc. London*, **40**, 187–99.
Hollister, L. S. (1969) *Bull. geol. Soc. Amer.* **80**, 2465–94.
——and Crawford, M. L. (1981) *Mineral. Assoc. Canada Short Course Handbook*, **6**, 304 pp.
Jacobs, G. K. and Kerrick, D. M. (1981) *Geochim. Cosmochim. Acta*, **45**, 607–14.
Kerrick, D. M. and Jacobs, G. K. (1981) *Amer. J. Sci.* **281**, 735–67.
Kowallis, B. J., Wang, H. F. and Jang, B. (1987) *Tectonophys.* **135**, 297–306.
Krantz, R. L. (1979*a*) *Int. J. Rock. Mech. Min. Sci.* **16**, 23–35.
——(1979*b*) Ibid. **16**, 37–47.
——(1983) *Tectonophys.* **100**, 449–80.
Laubach, S. E. (1989) *J. Struct. Geol.* **11**, 603–11.
Lespinasse, M. (1981) D.E.A. U.S.T.L. Montpellier, 69 pp.
——(1984) *Mem. Geol. Geochim. Uranium*, **8**, 200 pp.
——and Pécher, A. (1986) *J. Struct. Geol.* **8**, 169–80.
——and Cathelineau, M. (1990) *Tectnophys.* (in press).
Peng, S. and Johnson, A. M. (1972) *Int. J. Rock. Mech. Min. Sci.* **9**, 37–82.
Pécher, A., Lespinasse, M. and Leroy, J. (1985) *Lithos*, **18**, 229–37.
Potter, R. W. (1977) *J. Res. U.S. Geol. Surv.* **6**, 245–57.
——Clynne, M. A. and Brown, D. L. (1978) *Econ. Geol.* **73**, 284–5.
Poty, B., Leroy, J. and Jachimowicz, L. (1976) *Bull.* Soc. Fr. Mineral. Cristallogr. **99**, 182–6.

Ramboz, C., Schnapper, D. and Dubessy, J. (1985) *Geochim. Cosmochim. Acta*, **49**, 205–19.
Raynaud, S. (1979) Unpub. thesis U.S.T.L. Montpellier, 82 pp.
Ren, X., Kowallis, B. J. and Best, G. M. (1989) *Geology*, **17**, 487–90.
Roedder, E. (1962) *Econ. Geol.* **57**, 1045–61.
——(1972) *U.S. Geol. Surv., Prof Paper*, **440**, JJ, 164 pp.
——(1984) *Reviews in Mineralogy*, **12**, 644 pp. Min. Soc. America.
Seki, Y. (1961) *Jap. J. Geol. Geog.* **32**, 55–78.
Simmons, G. and Richter, D. (1976) Microcracks in rocks. In *The Physics and Chemistry of Rocks and Minerals* (Strens, R. G. J., ed.). Wiley, New York, 105–37.
Tapponier, P. and Brace, W. F. (1976) *Int. J. Rock. Mech. Min. Sci.* **13**, 103–12.
Tilley, C. E. (1924) *Q.J. Geol. Soc. Lond.* **80**, 22–70.
Tourte, J. (1977) *Thermodynamics in Geology* (Fraser, D. G., ed.) D. Reidel Publ. Co., Dordrecht, The Netherlands, 203–27.
Tuttle, O. F. (1949) *J. Geology*, **54**, 4, 331–56.
Van Hise, C. R. (1890) *Geol. Soc. Am. Bull.* **1**, 216–8.
Vergely, R. and Blanc, J. M. (1981) *C.R. Somm. Soc. Géol. Fr.* 167–70.
Virlogeux, D. (1984) Unpub. report C.F.M. Lozère, 84/06, 37.
Wise, D. U. (1964) *Geol. Soc. Am. Bull.* **75**, 287–306.

[*Revised manuscript received 1 December 1989*]